BJU Int 2026; **138:** 133–143 doi:10.1111/bju.70293

BJUI
BJU International

Original Article

Nodal maximum standardised uptake value improves PSMA-PET/CT-based nodal staging in intermediate- and high-risk prostate cancer

Alexandra S. Bruins Slot[1], Vera Sweere[1], Joris G. Heetman[1], Rick Hermsen[3], Lieke Wever[1], Jules Lavalaye[2], Maarten Vinken[3], Clinton D. Bahler[7], Mark Tann[8], Claudia Kesch[9], Tugce Telli[10,11,12], Wolfgang P. Fendler[10,11,12], Peter Ka-Fung Chiu[13], Kwan Kit Wu[14], Fabio Zattoni[15], Laura Evangelista[16,17], Francesco Ceci[18,19], Marcin Miszczyk[22,23], Pawel Rajwa[22,24,25], Akihiro Matsukawa[22,26], Tamás Fazekas[22,27], Francesco Barletta[20], Alberto Briganti[20], Francesco Montorsi[20], Giorgio Gandaglia[20], Jean-Paul A. Van Basten[4], Harm H. E. Van Melick[1], Roderick C. N. Van den Bergh[5], Giancarlo Marra[21], Timo F. W. Soeterik[1,6], Matthijs J. V. Scheltema[1] and on behalf of the European Association of Urology-Young Academic Urologists (EAU-YAU) Prostate Cancer Working Group

[1]Department of Urology, [2]Department of Nuclear Medicine, St. Antonius Hospital, Nieuwegein/Utrecht, [3]Department of Nuclear Medicine, [4]Department of Urology, Canisius Wilhelmina Hospital, Nijmegen, [5]Department of Urology, Erasmus Medical Center, Rotterdam, [6]Department of Radiation Oncology, University Medical Center Utrecht, Utrecht, The Netherlands, [7]Department of Urology, [8]Department of Radiology and Imaging Sciences, Indiana University Medical Center, Indianapolis, IN, USA, [9]Department of Urology, University Hospital Essen, Essen German Cancer Consortium (DKTK) University Hospital Essen, [10]Department of Nuclear Medicine, University Hospital Essen, [11]West German Cancer Center (WTZ), [12]German Cancer Consortium (DKTK), Essen, Germany, [13]S. H. Ho Urology Centre, Department of Surgery, The Chinese University of Hong Kong, [14]Department of Nuclear Medicine and PET, Hong Kong Sanatorium and Hospital, Hong Kong, China, [15]Urological Unit, Department of Surgery, Oncology, and Gastroenterology, University of Padova, Padova, [16]Department of Biomedical Sciences, Humanitas University, [17]Division of Nuclear Medicine, IRCCS Humanitas Research Hospital, [18]Division of Nuclear Medicine and Theranostics, IEO European Institute of Oncology, IRCCS, [19]Department of Oncology and Hemato-Oncology, University of Milan, [20]Division of Oncology/Unit of Urology, Soldera Prostate Cancer Lab, URI, IRCCS San Raffaele Scientific Institute, Vita-Salute San Raffaele University, Milan, [21]Division of Urology, Department of Surgical Sciences, Molinette Hospital, Città della Salute e della Scienza and University of Turin, Turin, Italy, [22]Department of Urology, Comprehensive Cancer Center, Medical University of Vienna, Vienna, Austria, [23]Collegium Medicum – Faculty of Medicine, WSB University, Dąbrowa Górnicza, [24]Second Department of Urology, Centre of Postgraduate Medical Education, Warsaw, Poland, [25]Division of Surgery and Interventional Science, University College London, London, UK, [26]Department of Urology, The Jikei University School of Medicine, Tokyo, Japan, and [27]Department of Urology, Semmelweis University, Budapest, Hungary

T.F.W.S. and M.J.V.S. shared senior authorship.

Objectives

To evaluate whether nodal maximum standardised uptake value (SUV_{max}) improves the positive predictive value (PPV) of prostate-specific membrane antigen (PSMA) positron emission tomography (PET)/computerised tomography (CT) for detecting lymph node invasion (LNI) in prostate cancer (PCa), and to develop clinical decision tools to guide decision-making for patients with low- and high-volume nodal disease.

Patients and Methods

This international multicentre study included patients with histopathologically confirmed PCa who underwent preoperative PSMA-PET and robot-assisted radical prostatectomy with extended pelvic lymph node dissection (2016–2023). Sensitivity, specificity, PPV, and negative predictive value (NPV) for LNI detection were calculated, defining a positive test as non-physiological PSMA uptake classified according to the Prostate Cancer Molecular Imaging Standardised Evaluation (PROMISE) molecular imaging Tumour-Node-Metastasis (miTNM) system. Receiver operating curves analysis identified optimal nodal SUV_{max} cut-offs for pelvic LNI. Logistic regression assessed predictors for pathological N1 stage (pN1) and high-volume nodal disease (four or more positive nodes). Clinical decision tools were developed to stratify patients into three risk groups for pN1 and high-volume nodal disease.

Results

A total of 521 patients were included, with a median (interquartile range) age of 66 (61–71) years and prostate-specific antigen (PSA) level of 9.9 (6.6–17.0) ng/mL. The PSMA-PET showed 45.0% sensitivity, 94.3% specificity, 64.7% PPV, and 88.3% NPV for LNI detection. Adding nodal SUV_{max} ≥4.9 improved the PPV to 81.1% and sensitivity to 71.4% and, combined with a PSA level ≥10 ng/mL, magnetic resonance imaging (MRI) T-stage ≥T3a, and miT-stage ≥T3a, identified 95% of pN1 cases in the high-risk group. High-volume nodal disease was found in 3.8%, including 1.1% in miN0 patients. Nodal SUV_{max} ≥7.2, MRI T-stage ≥T3a, and miN2 (multiple suspicious LNs) were predictors for high-volume nodal disease and, combined in a clinical decision tool, excluded all low-risk patients for high-volume nodal disease.

Conclusion

Nodal SUV_{max} improves PPV of PSMA-PET for nodal staging and aids in excluding high-volume nodal disease. Clinical decision tools integrating nodal SUV_{max} with relevant clinical parameters demonstrate potential to guide individualised nodal management. These findings warrant external validation in larger cohorts.

Keywords

Prostate-specific membrane antigen-positron emission tomography/computerised tomography, maximum standardised uptake value, prostatectomy, staging, lymph node invasion, high-volume nodal disease

Introduction

The presence of lymph node (LN) invasion (LNI) is an important prognostic factor in prostate cancer (PCa), as it is associated with higher risk of disease progression and mortality [1]. Prostate-specific membrane antigen (PSMA) positron emission tomography (PET)/CT has demonstrated superior diagnostic accuracy for nodal staging compared to conventional imaging (i.e., MRI and CT) [2]. However, PSMA-PET is still hampered by its suboptimal sensitivity (up to 57%) [3–5], likely due by its limited spatial resolution, which restricts the detection of micrometastatic disease [6]. Therefore, PSMA-PET may not fully replace extended pelvic LN dissection (ePLND) to assist pelvic nodal staging [4].

Despite its superior diagnostic performance, the specificity of PSMA-PET remains suboptimal, as not all patients with PSMA-avid LNs harbour histopathological positive LNs (pathological N stage [pN]1), supported by the positive predictive value (PPV) rates, varying from 54% to 77% in previous studies [4,5]. This implies that even in patients with node-positive PSMA-PET, risk stratification remains important. Therefore, it is crucial to determine whether additional PSMA-PET parameters could improve the PPV of molecular imaging (mi), ensuring that only those most likely to benefit from intensified treatment regiments are selected based on imaging results. Prior studies demonstrated strong association between intraprostatic maximum standardised uptake value (SUV_{max}) and histopathologically confirmed LNI [7,8]. Therefore, in line with previous data, we hypothesised that the absolute intranodal SUV_{max} values may also aid in LNI risk prediction [9,10].

This study aimed to evaluate whether nodal SUV_{max} is able to identify pN1 disease as well as high-volume nodal disease and therefore can enhance the PPV of preoperative PSMA-PET for nodal staging. In addition, we assessed the prevalence of high-volume nodal metastases in node-negative (miN0) and node-positive (miN+) disease to aid the development of two clinical decision tools for predicting pN1 and high-volume nodal disease, with the goal of providing a simple and practical tool for clinicians to support therapeutic decision-making in daily clinical practice.

Patients and Methods

Patient Selection

Men with histologically confirmed PCa, who underwent preoperative PSMA-PET and robot-assisted radical prostatectomy (RARP) with ePLND as treatment between 2016 and 2023 in seven tertiary referral centres were included in this retrospective observational study. Patients were excluded if they had received prior treatment for PCa or lacked complete PSMA-PET nodal staging data. This study represents a secondary analysis of the previously published observational study of Soeterik et al. [11]. Institutional Review Board approval was obtained before data collection (AW24.048/W18.055).

Data Collection

Clinical, imaging and pathological data were retrospectively collected. Preoperative variables included age, initial PSA, clinical tumour stage, D'Amico classification, MRI-derived

PSA density (PSAd), MRI tumour (MRI T)-stage, biopsy International Society of Urological Pathologists (ISUP) Grade Group (GG), molecular imaging tumour (miT)-stage, prostate SUV_{max}, nodal SUV_{max}, and molecular imaging nodal (miN)-stage. Postoperative parameters included pathological tumour stage (pT), RARP ISUP GG, pathological nodal stage (pN) with the total number of LNs resected and positive LNs, positive surgical margins, extracapsular extension and seminal vesical invasion.

Extended PLND Protocol

All ePLNDs were carried out by experienced urological surgeons. All centres utilised a standardised template including excision of lymphatic tissue along the internal iliac, external iliac and the obturator fossa. The lateral border was defined by the genitofemoralis nerve, the medial border by the bladder, the ureteric crossing as cranial border and the distal border by the obturator nerve [12].

Modifications to this dissection template, such as extension to a super-ePLND, were permitted based on the clinical judgement of the operating surgical team [13]. In all participating centres, histopathological evaluation was performed and reported by experienced uropathologists using the ISUP guidelines [14]. LNs were processed individually, and depending on local protocol, either one or multiple slides per LN were prepared.

Outcomes

The primary endpoints of this study were the sensitivity, specificity, PPV, and negative predictive value (NPV) of PSMA-PET for the detection of LNI on a per-patient basis and using histopathology as reference. Additionally, diagnostic accuracy of PSMA-PET in predicting pN1 as well as high-volume nodal disease was assessed using nodal SUV_{max}. The presence of high-volume nodal disease was analysed, with high-volume nodal disease defined as four or more histologically confirmed malignant loco-regional LNs. This definition has been applied in previous studies as a prognostic discriminator for nodal disease burden in relation to oncological outcomes and response to adjuvant therapy [15,16]. Finally, potential independent predictors associated with pN1 and high-volume nodal disease were examined and incorporated in clinical decision tools.

The PSMA-PET/CT

All PSMA-PET scans were conducted at tertiary centres following standardised local protocols. A detailed overview of these protocols has been described previously [11]. Additionally, PET scans performed externally for referred patients were included, provided they were re-evaluated by the local team. Molecular imaging was conducted from mid-thigh to skull base and combined with either a low-dose or a diagnostic CT scan for anatomical correlation. Experienced nuclear medicine physicians, defined as having >5 years of experience and/or having evaluated >500 scans, analysed all PSMA-PET scans. Radioligands use was based on specific centre preference, and included ^{18}F-PSMA-1007, ^{18}F-DCF-PyL, ^{18}F-JK-PSMA-7, and ^{68}Ga-PSMA-11. Image acquisition followed the guidelines established by the European Association of Nuclear Medicine (EANM) and the Society of Nuclear Medicine and Molecular Imaging (SNMMI) [17]. PSMA parameters were assessed as previously described [11]. LN metastases were defined as increased PSMA uptake, higher than the background, incompatible with physiological uptake, and in a typical site of PCa. In case of PSMA-PET suspicious LNs, nodal SUV_{max} was measured by the nuclear physician (i.e., the highest uptake value within a single voxel of the region of interest). Other PSMA parameters evaluated were intraprostatic SUV_{max}. Patients were categorised according to the nodal staging system of the Prostate Cancer Molecular Imaging Standardised Evaluation (PROMISE) criteria [18]: miN0 if no suspicious regional LNs were identified; miN1 if a single suspicious regional LN was detected; and miN2 if multiple suspicious regional LNs were present. For the purposes of this analysis, patients with miN1 or miN2 status were collectively classified as miN+.

Statistical Analysis

Differences between miN0 and miN+ patients were summarised using median values and interquartile ranges (IQRs) and compared using the Mann–Whitney *U* test for continuous variables and chi-square or Fisher's exact test for categorical variables. Patient-based sensitivity, specificity, PPV and NPV of PSMA-PET for LNI were calculated using a 2×2 contingency tables with histopathology as reference. Risk of nodal disease was estimated using either the Amsterdam-Brisbane-Sydney [19] or Briganti 2012 [20] nomograms, depending on data availability. In miN+ patients, associations between nodal SUV_{max} and pN1 disease were evaluated using univariate logistic regression, visual inspection of predicted probabilities (for all tracers and tracer-specific), and proportions of pN1 disease across nodal SUV_{max} cut-offs. Differences in proportions of pN1 disease across nodal SUV_{max} cut-offs were assessed using chi-square or Fisher's exact test. PSA and prostate SUV_{max} were also analysed using univariate logistic regression analyses. For continuous variables, area under the receiver operating characteristic curve analyses with Youden Index were applied to derive clinically applicable cut-offs for predicting pN1 disease. Multivariate models including PSA, prostate SUV_{max}, MRI T-stage ≥T3a, miT-stage ≥T3a, and biopsy GG ≥4 were constructed, both with and without nodal SUV_{max}, using backward elimination based on Akaike information criterion (AIC). Pearson's correlation coefficient analysis of variables

included in the final model was performed. In addition, multicollinearity was assessed by calculating variance inflation factors (VIFs), with a VIF >5 considered indicative of potential collinearity. A clinical decision tool was developed stratifying patients into low (no or one positive criterion), intermediate (two criteria), and high-risk (three or more criteria) for pN1 disease. Additionally, prevalence of high-volume nodal disease was analysed. High-volume nodal disease was defined as four or more histologically confirmed malignant loco-regional LNs, as the involvement of nodal burden may impact adjuvant treatment selection [15,16]. Statistical analyses described for pN1 as outcome were repeated for the outcome of high-volume nodal disease. All analyses were performed using two-sided tests, with a $P < 0.05$ considered statistically significant. Statistical analysis was performed using the IBM Statistical Package for the Social Sciences (SPSS®; IBM Corp. Version 29.0. Armonk, NY) and R version 4.4.0.

Results

Baseline Characteristics

This study included 521 patients who underwent RARP and ePLND. Table 1 highlights the significant differences between miN0 and miN+ patients. Of all patients, 86.9% were identified as miN0 and 13.1% as miN+. Within miN+ patients, 38 (55.9%) harboured one suspicious LN on PSMA-PET whereas 30 (44.1%) patients harboured multiple suspicious LNs. The median (IQR) risk of nodal disease was 14.0% (7.4–27.9%). The median (IQR) number of dissected LNs per patient was 16 (11–22). In all, 18.6% had histologically confirmed nodal disease. The median (IQR) age was 66 (61–71) years. The median (IQR) PSA level was 9.9 (6.6–17.0) ng/mL. The most common biopsy GG was 4 (28.4%). In 58.3% of patients, pT-stage was ≥T3a. The median prostate SUV_{max} was comparable between miN1 and miN2 disease (median [IQR] 11.3 [6.5–29.8] vs 16.5 [9.1–29.0]; $P = 0.239$). Similarly, the median nodal SUV_{max} did not differ between miN1 and miN2 patients (median [IQR] 5.1 [2.6–8.4] vs 5.6 [2.9–18.0]; $P = 0.430$). Sensitivity, specificity, PPV and NPV of PSMA-PET in detection of LNI were 45.0%, 94.3%, 64.7%, and 88.3%, respectively.

Differentiating Between pN0 and pN1 Disease in miN+

Uni- and Multivariate Association with Continuous Nodal SUV_{max}, PSA and Prostate SUV_{max}

In univariate analyses, higher nodal SUV_{max} (odds ratio [OR] 1.16, 95% CI 1.02–1.31; $P = 0.020$) and PSA (OR 1.11, 95% CI 1.04–1.23; $P = 0.016$) were significantly associated with LNI, whereas prostate SUV_{max} was not (Table S1). Fig. 1 and Tables S2 and S3 demonstrate a gradual increase in risk of pN1 disease with higher nodal SUV_{max}. This pattern is consistent across all tracers combined and within the ^{68}Ga-PSMA-11 and ^{18}F-PSMA-1007 subgroups. Table S1 showed multivariate logistic regression models with and without nodal SUV_{max}; inclusion of nodal SUV_{max} improved model performance (AIC decreased from 67.08 to 64.32), which was confirmed by likelihood ratio testing (chi-square = 4.85, $P = 0.028$).

Cut-offs and Dichotomised Univariate Association

Optimal cut-offs for predicting pN1 for PSA, prostate and nodal SUV_{max} were ≥10 ng/mL, ≥15 and ≥4.9, respectively (Table S4). In patients who are judged to have miN+ disease by the readers, nodal SUV_{max} ≥4.9 resulted in sensitivity, specificity, PPV and NPV for LN detection of 71.4%, 68.2%, 81.1%, and 55.6%, respectively. Additionally, a significantly higher proportion of patients with nodal SUV_{max} ≥4.9 (81.1%) harboured pN1 compared to those <4.9 (44.4%) ($P = 0.003$). Tables S2 and S3 present results of additional cut-offs. A PSA level ≥10 ng/mL, nodal SUV_{max} ≥4.9, MRI T-stage ≥T3a and miT-stage ≥T3a were significantly associated with nodal disease in univariate analyses (Table 2).

Dichotomised Multivariate Logistic Regression and Clinical Decision Tool

The final multivariate model incorporated PSA level ≥10 ng/mL, nodal SUV_{max} ≥4.9, MRI T-stage ≥T3a and miT-stage ≥T3a (Table 2). This final model demonstrated a lower AIC compared to the first model, which incorporated all variables included in univariate analysis (64.6 vs 69.2). Correlation analysis showed a weak correlation between MRI T-stage and miT-stage ($r = 0.129$), and corresponding VIF (1.017) confirmed the absence of multicollinearity.

A clinical decision tool was conducted incorporating PSA level ≥10 ng/mL, MRI T-stage ≥T3a, miT-stage ≥T3a and nodal SUV_{max} ≥4.9. In this study, 36.8%, 26.3% and 36.8% of patients were classified as low-, intermediate- and high-risk of pN1. In patients classified as high-risk, 95% (20 of 21 patients) harboured pN1 disease, compared to 29% (six of 21) if classified as low-risk ($P < 0.001$), as presented in Table S5A.

High-Volume Nodal Disease

Characteristics for High-Volume Nodal Disease for miN0 and miN+ Patients

High-volume nodal disease was present in 3.8% of patients. Among miN0, high-volume nodal disease was histologically confirmed in 1.1% (five of 453 patients), while this was 22.1%

Table 1 Patients' characteristics for all patients, and miN0 compared with miN+.

Characteristic	All patients (*n* = 521)	miN0 (*n* = 453)	miN+ (*n* = 68)	*P*
Age, years, median (IQR)	66.0 (61.0–71.0)	66.0 (61.0–71.0)	66.5 (60.5–72.0)	0.826
PSA level, ng/mL, median (IQR)	9.9 (6.6–17.0)	9.7 (6.4–16.5)	12.1 (8.0–21.2)	**0.006**
Clinical T-stage, *n* (%)				
≤T2a	401 (77.0)	349 (77.0)	52 (76.5)	0.367
T2b	33 (6.3)	30 (6.6)	3 (4.4)	
T2c	12 (2.3)	12 (2.6)	0 (0.0)	
≥T3	67 (12.9)	55 (12.1)	12 (17.6)	
Missing	8 (1.5)	7 (1.5)	0 (0.0)	
D'Amico classification, *n* (%)				
Low risk	4 (0.8)	4 (0.9)	0 (0.0)	**0.028**
Intermediate risk	202 (38.8)	185 (40.8)	17 (25.0)	
High risk	315 (60.5)	264 (58.3)	51 (75.0)	
MRI-derived PSAd, ng/mL/mL, median (IQR)	0.215 (0.131–0.371)	0.212 (0.126–0.364)	0.236 (0.157–0.406)	0.248
MRI T-stage, *n* (%)				
≤T2c	259 (49.7)	231 (51.0)	28 (41.1)	0.078
T3a	165 (31.7)	146 (32.2)	19 (27.9)	
T3b	57 (10.9)	43 (9.5)	14 (20.6)	
T4	2 (0.4)	2 (0.5)	0 (0.0)	
No MRI	38 (7.3)	31 (6.8)	7 (10.3)	
Biopsy GG, *n* (%)				
≤1	18 (3.5)	17 (3.8)	1 (1.5)	**0.003**
2	118 (22.6)	108 (23.8)	10 (14.7)	
3	143 (27.4)	130 (28.7)	13 (19.1)	
4	148 (28.4)	128 (28.3)	20 (29.4)	
5	93 (17.9)	69 (15.2)	24 (35.3)	
Missing	1 (0.2)	1 (0.2)	0 (0.0)	
miT-stage, *n* (%)				
miT0	28 (5.4)	25 (5.5)	3 (4.4)	**0.003**
miT2	304 (58.3)	272 (60.0)	32 (47.1)	
miT3a	138 (26.5)	120 (26.5)	18 (26.5)	
miT3b	29 (5.6)	21 (4.6)	8 (11.8)	
miT4	10 (1.9)	5 (1.1)	5 (7.4)	
Missing	12 (2.3)	10 (2.2)	2 (0.0)	
Highest prostate SUV_{max}, median (IQR)	10.2 (6.3–17.6)	9.9 (6.2–16.2)	13.6 (7.0–29.6)	**0.002**
Highest nodal SUV_{max}, median (IQR)	0 (0–2.6)	NA	5.2 (2.8–9.6)	NA
pT-stage, *n* (%)				
pT2	216 (41.7)	207 (45.7)	9 (13.2)	<**0.001**
pT3a	180 (34.5)	153 (33.8)	27 (39.7)	
pT3b	122 (23.4)	90 (19.9)	32 (47.1)	
pT4	2 (0.4)	2 (0.4)	0 (0.0)	
Missing	1 (0.2)	1 (0.2)	0 (0.0)	
RARP GG, *n* (%)				
1	8 (1.5)	6 (1.3)	2 (2.9)	<**0.001**
2	187 (35.9)	176 (38.9)	11 (16.2)	
3	194 (37.2)	171 (37.7)	23 (33.8)	
4	54 (10.4)	48 (10.6)	6 (8.8)	
5	74 (14.2)	48 (10.6)	26 (38.2)	
Missing	4 (0.8)	4 (0.9)	0 (0.0)	
pN-stage, *n* (%)				
pN0	424 (81.4)	400 (88.3)	24 (35.3)	<**0.001**
pN1	97 (18.6)	53 (11.7)	44 (64.7)	
LNs resected, *n*, median (IQR)	16.0 (11.0–22.0)	16.0 (10.0–22.0)	22.0 (14.5–26.8)	<**0.001**
Positive LNs, median (IQR)	0.0 (0.0–0.0)	0.0 (0.0–0.0)	1.5 (0.0–2.8)	<**0.001**
0, *n* (%)	424 (81.4)	400 (88.3)	24 (35.3)	<**0.001**
1, *n* (%)	46 (8.8)	36 (7.9)	10 (14.7)	
2, *n* (%)	26 (5.0)	9 (2.0)	17 (25.0)	
3, *n* (%)	5 (1.0)	3 (0.7)	2 (2.9)	
≥4, *n* (%)	20 (3.8)	5 (1.1)	15 (22.1)	
Positive surgical margin, *n* (%)				
No	351 (67.4)	310 (68.4)	41 (60.3)	0.078
Yes	168 (32.2)	141 (31.2)	27 (39.7)	
Missing	2 (0.4)	2 (0.4)	0 (0.0)	
Extracapsular extension, *n* (%)				
No	238 (45.7)	224 (49.4)	14 (20.6)	<**0.001**
Yes	276 (53.0)	223 (49.2)	53 (78.0)	
Missing	7 (1.4)	6 (1.3)	1 (1.5)	

Table 1 (continued)

Characteristic	All patients (*n* = 521)	miN0 (*n* = 453)	miN+ (*n* = 68)	*P*
Seminal vesical invasion, *n* (%)				
No	385 (73.9)	352 (77.7)	33 (48.5)	**<0.001**
Yes	109 (21.0)	79 (17.5)	30 (44.1)	
Missing	27 (5.2)	22 (4.8)	5 (7.4)	

Bold values statistically significant at P < 0.05.

Fig. 1 Relationship between nodal SUV_{max} and pN1 disease. **(A)** All tracers included. **(B)** ^{68}Ga-PSMA-11. **(C)** ^{18}F-PSMA-1007. **(D)** ^{18}F-DCF-PyL.

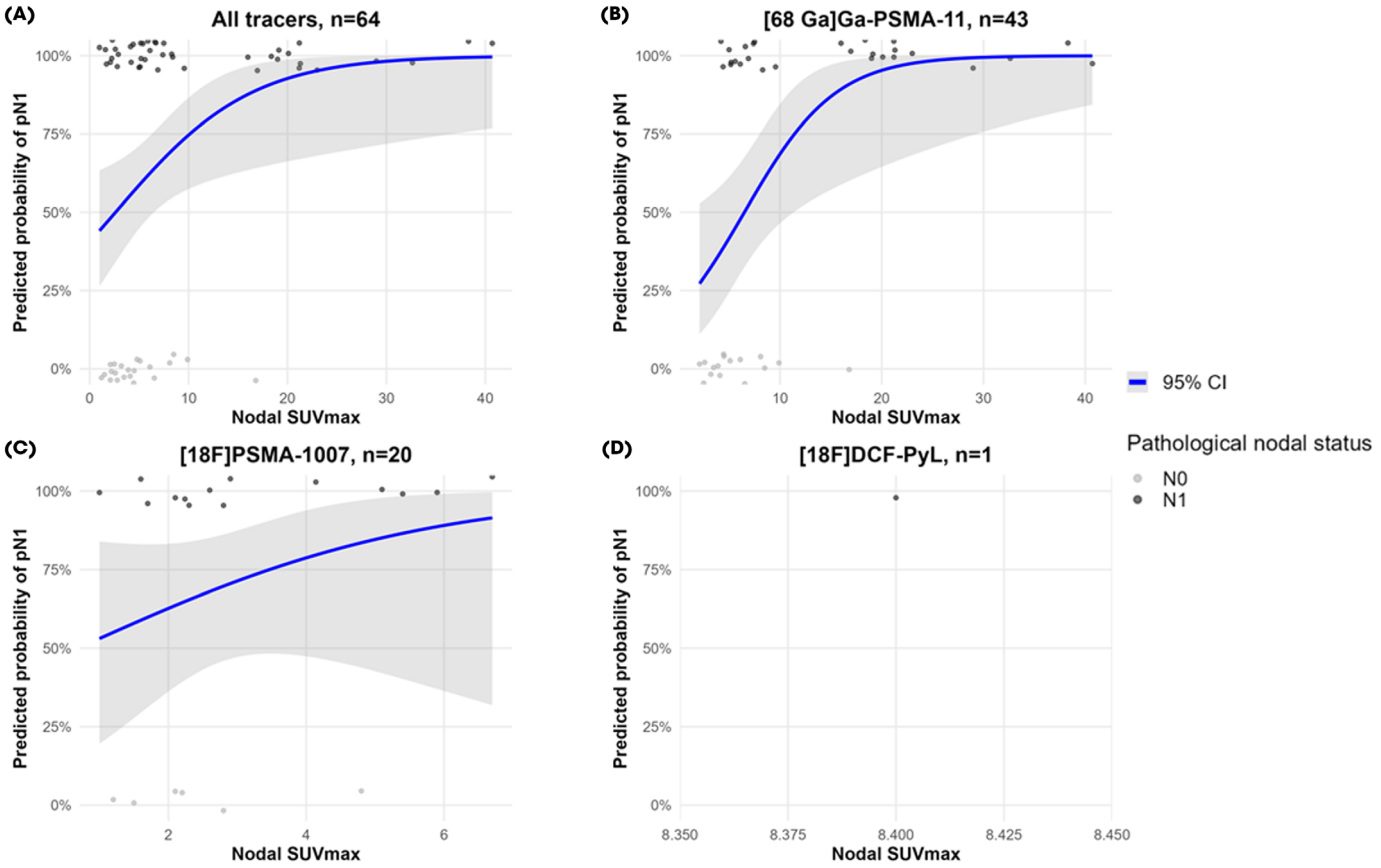

(15 of 68) in miN+ patients. In miN1 disease, this was 7.9% (three of 38 patients) and in miN2 patients 40.0% (12 of 30). Patient characteristics are shown in Table S6.

Continuous Univariate Logistic Regression Analyses

In univariate logistic regression analyses, there was no significant association with high-volume nodal disease for nodal SUV_{max} (OR 1.057, 95% CI 0.996–1.121; $P = 0.069$), prostate SUV_{max} (OR 0.996, 95% CI 0.965–1.028; $P = 0.799$) and PSA level (OR 1.019, 95% CI 0.995–1.043; $P = 0.120$).

Cut-offs and Dichotomised Univariate Association

Optimal cut-offs for predicting high-volume nodal disease for PSA level, prostate and nodal SUV_{max} were ≥16.4 ng/mL, ≥16.2 and ≥7.2, respectively (Table S7). Nodal SUV_{max} of ≥7.2 resulted in a 60.0% sensitivity, 71.4% specificity, 39.1% PPV and 85.4% NPV. Furthermore, high-volume nodal disease was associated with a significantly higher proportion of patients with nodal SUV_{max} ≥7.2 (39.1%) compared to those with nodal SUV_{max} <7.2 (14.6%) ($P = 0.035$). In Tables S8 and S9, additional cut-offs and corresponding diagnostic accuracies are reported. A PSA level ≥16.4 ng/mL,

Table 2 Dichotomised uni- and multivariate logistic regression analyses to assess predictors for pN1 disease.

Variables	OR (95% CI)	*P*	AIC
Univariate logistic regression analyses			
PSA level ≥10 ng/mL	6.476 (2.234–20.631)	**0.001**	80.04
Prostate SUV_{max} ≥15	2.400 (0.870–7.022)	0.098	89.45
Nodal SUV_{max} ≥4.9	5.357 (1.809–17.305)	**0.003**	76.99
MRI T-stage ≥T3a	3.606 (1.244–11.159)	**0.021**	79.23
miT-stage ≥T3a	4.333 (1.501–13.960)	**0.009**	84.79
Biopsy GG ≥4	0.875 (0.298–2.466)	0.803	92.24
Multivariate logistic regression analysis			
PSA level ≥10 ng/mL	4.093 (1.135–16.579)	0.037	64.61
Nodal SUV_{max} ≥4.9	4.152 (1.134–17.159)	**0.037**	64.61
MRI T-stage ≥T3a	3.132 (0.853–12.803)	0.093	64.61
miT-stage ≥T3a	3.869 (1.014–17.044)	0.056	64.61

Bold values statistically significant at P < 0.05.

Table 3 Uni- and multivariate logistic regression analyses to assess predictors for high-volume LNM disease.

Variables	OR (95% CI)	*P*	AIC
Univariate logistic regression analyses			
PSA level ≥16.4 ng/mL	4.179 (1.259–13.873)	**0.020**	70.13
Prostate SUV_{max} ≥16.2	1.741 (0.549–5.523)	0.346	74.87
Nodal SUV_{max} ≥7.2	3.750 (1.124–12.509)	**0.032**	68.93
MRI T-stage ≥T3a	4.875 (0.956–24.870)	0.057	57.08
miT-stage ≥T3a	2.818 (0.845–9.399)	0.092	72.76
miN2	7.778 (2.152–37.444)	**0.004**	65.37
ISUP GG biopsies GG ≥4	1.118 (0.333–3.753)	0.857	75.73
Multivariate logistic regression analysis			
Nodal SUV_{max} ≥7.2	4.544 (0.874–29.334)	0.083	48.18
MRI T-stage ≥T3a	6.140 (0.940–68.096)	0.084	48.18
miN2	14.903 (2.418–173.617)	**0.010**	48.18
ISUP GG biopsies GG ≥4	0.187 (0.020–1.139)	0.091	48.18

Bold values statistically significant at P < 0.05.

nodal SUV_{max} ≥7.2, and miN2 were significantly associated with high-volume nodal disease in univariate analyses (Table 3).

Multivariate Logistic Regression and Clinical Decision Tool

The final multivariate model, that included nodal SUV_{max} ≥7.2, MRI T-stage ≥T3a and miN2, demonstrated a lower AIC compared to the first model (52.7 vs 48.2), which incorporated all variables included in univariate analysis. All uni- and multivariate logistic regression results are summarised in Table 3.

The clinical decision tool for high-volume nodal disease prediction incorporated nodal SUV_{max} ≥7.2, MRI T-stage ≥T3a and miN2-stage. Low-, intermediate-, and high-risk groups comprised 22.8%, 63.2% and 14.0% of patients, respectively. In the low-risk group, no high-volume nodal disease (none of the 11 patients) was observed, compared to five of eight patients (63%) in the high-risk group ($P = 0.003$), as presented in Table S5B.

Discussion

This multicentre study is the first to evaluate predictors that can improve the accuracy of PSMA-PET to detect both pN1 and high-volume nodal disease. Additionally, we report on histopathological prevalence of high-volume nodal disease, in both miN0 and miN+ disease. Two clinical decision tools were generated to support clinicians in identifying patients at risk of pN1 or high-volume nodal disease, aiming to guide treatment decisions in routine practice.

Preoperative PSMA-PET showed high specificity (94.3%) and NPV (88.3%), but moderate sensitivity (45.0%) and PPV (64.7%) for detecting LNI in patients with intermediate- and high-risk PCa. These results are consistent with existing literature [3–5] and highlight the need for accurate preoperative nodal staging. What our study adds, is that we demonstrated a direct proportional association between nodal SUV_{max} and pN1 disease, both in the tracer-combined cohort and consistently across tracer-specific analyses. In addition, we presented the association between sensitivity and specificity for the detection of pN1, per SUV_{max} cut-off. While these cut-offs may improve clinical decision-making, they should be interpreted depending on patient characteristics and preferences, when determining the indication for PLND. Although no universally accepted SUV_{max} threshold exists, a nodal SUV_{max} of ≥4.9 emerged as a pragmatic cut-off when combined with clinical and imaging parameters, enabling effective risk stratification and identifying a subgroup with a very high likelihood of pelvic LN metastases. Applying this cut-off increased sensitivity to 71.4% and PPV to 81.1%, and patients with ≥4.9 were significantly more likely to harbour pN1 disease compared to those below this threshold (81.1% vs 44.4%, $P = 0.003$). While previous studies reported lower SUV_{max} cut-offs (>0.85 and >2), methodological differences and smaller sample sizes may explain discrepancies [21,22]. Arçay Öztürk et al. [23] found a similar cut-off of 4.72, although their analysis included primary, re-staging and response-monitoring PSMA-PET scans, limiting direct comparison with our cohort. Finally, Uprimny et al. [24] reported a median nodal SUV_{max} of 10.6 (range 3.1–90.6) among patients with pN1 but did not report a cut-off.

The clinical decision tool for predicting pN1 disease stratified patients into three risk groups. In all, 95% of the high-risk group harboured pN1 disease compared to only 29% in the low-risk group ($P < 0.001$). This suggest that the proposed tool may improve prediction of pN1 disease in patients with suspicious LNs on PSMA-PET and may therefore aid clinicians in refining treatment decision-making. For example,

patients in the high-risk group may be considered suitable candidates for whole pelvis radiotherapy (WPRT), given the high likelihood of nodal involvement and subsequent need of multimodality treatment. In contrast, those classified as low- or intermediate-risk, where the prevalence of pN1 disease was 29% and 67%, respectively, may benefit from additional surgical nodal staging via ePLND or sentinel node dissection (SND) [25], as nodal involvement in these groups remain uncertain. Although promising results, these findings warrant prospective validation.

Furthermore, our study offers novel insights into the prediction of high-volume nodal disease, as studies reporting the total nodal burden in miN+ patients selected for ePLND are scarce. This is clinically relevant, as high-volume nodal disease carries therapeutic implications: patients with four or more positive LNs may derive limited survival benefit from adjuvant RT [15,16]. However, due to the inclusion period of these studies, only a minority underwent PSMA-PET. This may impact RT results, as PSMA is superior compared to conventional imaging in finding positive LNs [2]. Moreover, PSMA-PET has been shown to change salvage RT (SRT) planning in 56.4% (pooled analysis) and has been associated with PSA or imaging response rates varying from 60% to 83%, which is higher when using conventional imaging [26,27]. In the ongoing PSMA-SRT randomised controlled trial, PSMA-PET led to change in SRT planning in 33% of patients. However, the trial's primary endpoint, whether PSMA-guided planning improves 5-year biochemical recurrence-free survival, has yet to be reported [28].

We observed a 3.8% prevalence of high-volume nodal disease, including 22.1% in miN+ patients and only 1.1% in miN0 patients, suggesting excellent performance of PSMA-PET in ruling out extensive nodal disease in miN0 disease. Van Leeuwen et al. [21] reported that, among 11 patients with LNI, only one miN+ patient had high-volume nodal disease, while all miN0 cases harboured a single positive LN. Erdem et al. [29] found high-volume nodal disease in one of five miN+ cases, while all miN0 cases had low-volume disease. However, these studies included small sample sizes and were not designed to assess the extent of nodal burden specifically. As this study proved that PSMA-PET is excellent in ruling out high-volume nodal disease in miN0 patients, low-volume LNI cannot be ruled out as previously described [4] and therefore surgical staging before applying (adjuvant) RT may be still necessary [16]. These patients could therefore opt for limited surgical nodal staging such as SND instead of ePLND treatment. SND is based on primary tumour lymphatic drainage and has demonstrated a 95.2% pooled sensitivity [25] and lower complication rates compared to ePLND [30].

Nodal SUV_{max} ≥7.2 was identified as optimal cut-off for predicting high-volume nodal disease in miN+ patients, achieving a sensitivity of 60% and NPV of 85.4%. Despite a modest PPV (39.1%), the absence of high-volume nodal disease in the low-risk group (0%) compared to 63% in the high-risk group underlines the potential value of this clinical decision tool in ruling out extensive nodal disease ($P = 0.035$). These findings suggest that the decision tool could support clinical decisions in preventing adjuvant therapy in the low-risk group.

To our knowledge, this is the first large multicentre study evaluating nodal SUV_{max} performance in identifying pN1 disease as well as high-volume nodal disease in patients with suspicious LNs on PSMA-PET. Two clinically applicable and easily interpretable decision tools were developed aiming to help in guiding treatment decisions. SUV_{max} has demonstrated low interobserver variability in a multicentre setting, establishing it as a robust and reproducible quantitative parameter for clinical decision-making [31].

This study has several limitations. First, selection bias may be present, as only patients undergoing both PSMA-PET and RARP with ePLND were included, excluding those with extensive nodal or distant disease. This limits generalisability and may overestimate specificity while underestimating sensitivity, particularly for LNs outside the surgical template [12]. Second, PSAd was not included in our analysis; although prognostically relevant, it was not significantly associated with pN1 or high-volume nodal disease in additional analyses (Table S10), and MRI-derived prostate volume was unavailable in ~20% of patients. Third, analysis was conducted on a per-patient rather than per-LN level, capturing only the highest nodal SUV_{max} per patient and potentially overlooking uptake heterogeneity. Fourth, physiological uptake was not reported, precluding direct comparison with background activity. Fifth, absence of centralised review for imaging and histopathology, may have introduced interobserver variability, although this makes the model more robust. Additionally, while all PSMA-PET adhered to EANM/SNMMI guidelines [17], variability in radioligands, imaging protocols and reconstructions across centres may still affect generalisability. Therefore, we performed an additional tracer-specific analysis (Table S11). While this suggested that inter-tracer variation may influence absolute SUV_{max} cut-offs, small subgroup sizes and inter-centre variability in PSMA-PET procedures and patient selection precluded definitive conclusions. At the same time, inclusion of multiple radioligands in our primary analysis reflected real-world practice variation. Future studies should investigate these differences more systematically to optimise diagnostic accuracy and support clinical decision-making. Moreover, prevalence of suspicious LNs on PSMA-PET and (histological) high-volume nodal disease was limited, therefore results should be interpreted with caution. In particular, analyses regarding high-volume nodal disease were exploratory and hypothesis-generating due to limited number

of patients (n = 20), which substantially limits statistical power and model stability. In addition, miN2 patients may have undergone a more extended ePLND, therefore incorporating miN2 as predictor in the decision tool may potentially have introduced verification bias. Nevertheless, identifying patients with extensive nodal burden remains clinically relevant, therefore these analyses were retained to provide preliminary hypotheses for future validation. Consequently, findings related to high-volume disease should be viewed as provisional and require confirmation in larger, prospectively enrolled cohorts. Additionally, although histopathology of ePLND served as reference standard for nodal involvement, it may fail to identify all metastatic LNs [12]. Finally, we did not perform internal validation, which introduces the possibility of overfitting. Further studies with larger, prospectively enrolled cohorts are needed to validate these findings and refine the proposed clinical decision tools.

Conclusions

In our multicentre study, PSMA-PET showed a 45.0% sensitivity, 94.3% specificity, 64.7% PPV, and 88.3% NPV for detection of nodal disease. Incorporating nodal SUV_{max} ≥4.9 to visual assessment increased sensitivity to 71.4% and PPV to 81.1%. The developed pN1 tool suggests a potential to identify those likely to harbour nodal disease, in whom WPRT may be considered instead of surgical staging. In addition, PSMA-PET effectively ruled out high-volume nodal disease, with only 1.1% of miN0 patients showing four or more positive LNs on histopathology. The high-volume nodal disease tool identified those patients without four or more positive nodes; however, analyses regarding high-volume disease were exploratory due to the limited sample size. Both tools require validation in larger prospective cohorts.

Acknowledgements

Marcin Miszczyk was supported by the European Urological Scholarship Programme (EUSP) Scholarship of the European Association of Urology (EAU). Paweł Rajwa was supported by NAWA – Polish National Agency for Academic Exchange in cooperation with Medical Research Agency under the Walczak Programme, grant number BPN/WAL/2023/1/00016.

Disclosure of Interests

Rick Hermsen received consultancy fees from ABX advance biochemical compounds GmbH and Blue Earth Diagnostics. Wolfgang P. Fendler reports fees from SOFIE Bioscience (research funding), Janssen (consultant, speaker), Perceptive (consultant, image review), Bayer (consultant, speaker, research funding), Novartis (speaker, consultant), Telix (speaker), GE Healthcare (speaker, consultant), Eczacıbaşı Monrol (speaker), Abx (speaker), Amgen (speaker), Urotrials (speaker), Lilly (consultant), AstraZeneca (research funding) outside of the submitted work. The remaining authors have no disclosures.

Funding

The authors declare that no funds, grants or other support were received during the preparation of this manuscript.

References

1 **Bernstein AN, Shoag JE, Golan R et al.** Contemporary incidence and outcomes of prostate cancer lymph node metastases. *J Urol* 2018; 199: 1510–7

2 **Chow KM, So WZ, Lee HJ et al.** Head-to-head comparison of the diagnostic accuracy of prostate-specific membrane antigen positron emission tomography and conventional imaging modalities for initial staging of intermediate- to high-risk prostate cancer: a systematic review and meta-analysis. *Eur Urol* 2023; 84: 36–48

3 **Jeet V, Parkinson B, Song R, Sharma R, Hoyle M.** Histopathologically validated diagnostic accuracy of PSMA-PET/CT in the primary and secondary staging of prostate cancer and the impact of PSMA-PET/CT on clinical management: a systematic review and meta-analysis. *Semin Nucl Med* 2023; 53: 706–18

4 **van Kalmthout L, van Melick H, Lavalaye J et al.** Prospective validation of Gallium-68 prostate specific membrane antigen-positron emission tomography/computerized tomography for primary staging of prostate cancer. *J Urol* 2020; 203: 537–45

5 **Jansen BHE, Bodar YJL, Zwezerijnen GJC et al.** Pelvic lymph-node staging with 18F-DCFPyL PET/CT prior to extended pelvic lymph-node dissection in primary prostate cancer – the SALT trial. *Eur J Nucl Med Mol Imaging* 2021; 48: 509–20

6 **Jilg CA, Drendel V, Rischke C et al.** Diagnostic accuracy of Ga-68-HBED-CC-PSMA-ligand-PET/CT before salvage lymph node dissection for recurrent prostate cancer. *Theranostics* 2017; 7: 1770–80

7 **Roberts MJ, Morton A, Donato P et al.** 68Ga-PSMA PET/CT tumour intensity pre-operatively predicts adverse pathological outcomes and progression-free survival in localised prostate cancer. *Eur J Nucl Med Mol Imaging* 2021; 48: 477–82

8 **Bodar YJL, Veerman H, Meijer D et al.** Standardised uptake values as determined on prostate-specific membrane antigen positron emission tomography/computed tomography is associated with oncological outcomes in patients with prostate cancer. *BJU Int* 2022; 129: 768–76

9 **Kurash MM, Gill R, Khairulin M et al.** 68Ga-labeled PSMA-11 (68Ga-isoPROtrace-11) synthesized with ready to use kit: normal biodistribution and uptake characteristics of tumour lesions. *Sci Rep* 2020; 10: 1–8

10 **Cytawa W, Seitz AK, Kircher S et al.** A prospective study to assess the diagnostic accuracy and management impact of prostate specific membrane antigen (PSMA) PET scanning in men with prostate cancer being considered for surgery or radiotherapy. *Eur J Nucl Med Mol Imaging* 2020; 47: 168–77

11 **Soeterik TFW, Heetman JG, Hermsen R et al.** The association of quantitative PSMA PET parameters with pathologic ISUP grade: an international multicenter analysis. *Eur J Nucl Med Mol Imaging* 2024; 52: 314–25

12 **Mattei A, Fuechsel FG, Bhatta Dhar N et al.** The template of the primary lymphatic landing sites of the prostate should be revisited: results of a multimodality mapping study. *Eur Urol* 2008; 53: 118–25

13 **Baas DJH, de Baaij JMS, Sedelaar JPM et al.** Extended pelvic lymph node dissection in robot-assisted radical prostatectomy is an independent risk factor for major complications. *J Robot Surg* 2024; 18: 1–10

14 **Berney DM, Wheeler TM, Grignon DJ et al.** International society of urological pathology (ISUP) consensus conference on handling and

staging of radical prostatectomy specimens. Working group 4: seminal vesicles and lymph nodes. *Mod Pathol* 2011; 24: 39–47

15 **Tilki D, Chen M-H, Wu J, Huland H, Graefen M, D'Amico AV.** Adjuvant versus early salvage radiation therapy after radical prostatectomy for pN1 prostate cancer and the risk of death. *J Clin Oncol* 2022; 40: 2186–92

16 **Abdollah F, Karnes RJ, Suardi N et al.** Impact of adjuvant radiotherapy on survival of patients with node-positive prostate cancer. *J Clin Oncol* 2014; 32: 3939–47

17 **Fendler WP, Eiber M, Beheshti M et al.** PSMA PET/CT: joint EANM procedure guideline/SNMMI procedure standard for prostate cancer imaging 2.0. *Eur J Nucl Med Mol Imaging* 2023; 50: 1466–86

18 **Seifert R, Emmett L, Rowe SP et al.** Second version of the prostate cancer molecular imaging standardized evaluation framework including response evaluation for clinical trials (PROMISE V2). *Eur Urol* 2023; 83: 405–12

19 **Vis AN, Meijer D, Roberts MJ et al.** Development and external validation of a novel nomogram to predict the probability of pelvic lymph-node metastases in prostate cancer patients using magnetic resonance imaging and molecular imaging with prostate-specific membrane antigen positron emission. *Eur Urol Oncol* 2023; 6: 553–63

20 **Briganti A, Larcher A, Abdollah F et al.** Updated nomogram predicting lymph node invasion in patients with prostate cancer undergoing extended pelvic lymph node dissection: the essential importance of percentage of positive cores. *Eur Urol* 2012; 61: 480–7

21 **van Leeuwen PJ, Emmett L, Ho B et al.** Prospective evaluation of 68Gallium-prostate-specific membrane antigen positron emission tomography/computed tomography for preoperative lymph node staging in prostate cancer. *BJU Int* 2017; 119: 209–15

22 **Pratik TP, Sakthivel DK, Madhav TS et al.** Correlation of gallium-68 prostate-specific membrane antigen positron emission tomography – computed tomography/magnetic resonance imaging with histopathology characteristics in carcinoma prostate patients undergoing radical prostatectomy. *Indian J Urol* 2025; 41: 40–4

23 **Arçay Öztürk A, Erkılıç M, Bural GG, Aydın F, Boz A.** Physiological biodistribution on Ga68-PSMA PET/CT and the factors effecting biodistribution. *Ann Nucl Med* 2024; 38: 894–903

24 **Uprimny C, Kroiss AS, Decristoforo C et al.** 68Ga-PSMA-11 PET/CT in primary staging of prostate cancer: PSA and Gleason score predict the intensity of tracer accumulation in the primary tumour. *Eur J Nucl Med Mol Imaging* 2017; 44: 941–9

25 **Wit EMK, Acar C, Grivas N et al.** Sentinel node procedure in prostate cancer: a systematic review to assess diagnostic accuracy. *Eur Urol* 2017; 71: 596–605

26 **Pozdnyakov A, Kulanthaivelu R, Bauman G, Ortega C, Veit-Haibach P, Metser U.** The impact of PSMA PET on the treatment and outcomes of men with biochemical recurrence of prostate cancer: a systematic review and meta-analysis. *Prostate Cancer Prostatic Dis* 2023; 26: 240–8

27 **Zaorsky NG, Calais J, Fanti S et al.** Salvage therapy for prostate cancer after radical prostatectomy. *Nat Rev Urol* 2021; 18: 643–68

28 **Armstrong WR, Kishan AU, Booker KM et al.** Impact of prostate-specific membrane antigen positron emission tomography/computed tomography on prostate cancer salvage radiotherapy management: results from a prospective multicenter randomized phase 3 trial (PSMA-SRT NCT03582774). *Eur Urol* 2024; 86: 52–60

29 **Erdem S, Simsek DH, Degirmenci E et al.** How accurate is 68Gallium-prostate specific membrane antigen positron emission tomography/computed tomography (68Ga-PSMA PET/CT) on primary lymph node staging before radical prostatectomy in intermediate and high risk prostate cancer? A study of patient. *Urol Oncol Semin Orig Investig* 2022; 40: 6.e1–6.e9

30 **de Barros HA, Duin JJ, Mulder D et al.** Sentinel node procedure to select clinically localized prostate cancer patients with occult nodal metastases for whole pelvis radiotherapy. *Eur Urol Open Sci* 2023; 49: 80–9

31 **Donswijk ML, Ettema RH, van der Gaag S et al.** The intra- and interobserver variability of PSMA-expression scores in patients with primary prostate cancer. *EJNMMI Res* 2024; 14: 99

Correspondence: Alexandra S. Bruins Slot, Department of Urology, St. Antonius Hospital, Koekoekslaan 1, 3435 CM Nieuwegein, The Netherlands. e-mail: a.bruins.slot@antoniusziekenhuis.nl

Abbreviations: AIC, Akaike information criterion; EANM, European Association of Nuclear Medicine; GG, Grade Group; IQR, interquartile range; ISUP, International Society of Urological Pathologists; LN, lymph node; LNI, LN invasion; mi, molecular imaging; OR, odds ratio; PCa, prostate cancer; PET, positron emission tomography; (e) PLND, (extended) pelvic LN dissection; pN, pathological N stage; PSAd, PSA density; PSMA, prostate-specific membrane antigen; pT, pathological tumour stage; (N)(P)PV, (negative) (positive) predictive value; RARP, robot-assisted radical prostatectomy; (S)(WP)RT, (salvage) (whole pelvis) radiotherapy; SND, sentinel node dissection; SNMMI, Society of Nuclear Medicine and Molecular Imaging; $SUV_{(max)}$, (maximum) standardised uptake value; VIF, variance inflation factor.

Supporting Information

Additional Supporting Information may be found in the online version of this article:

Table S1. Continuous uni- and multivariate logistic regression analyses to assess predictors for pN1 disease.

Table S2. Various nodal SUV_{max} cut-offs (after visual miN+) with corresponding diagnostic accuracy for distinguishing between pN0 and pN1 disease in miN+ patients.

Table S3. Proportion of miN+ patients with pN0 or pN1 disease based on various nodal SUV_{max} cut-offs.

Table S4. Receiver operating characteristic curve analyses for optimal cutoff values for predicting pN1.

Table S5. (A) proportion of patients with pN0 vs. pN1 disease stratified by risk group. (B) proportion of patients with 0–3 positive lymph nodes vs. ≥4 positive lymph nodes stratified by risk group.

Table S6. Characteristics of patients with high-volume LNM disease, stratified by miN-stage.

Table S7. Receiver operating characteristic curve analyses for optimal cutoff for predicting high volume nodal disease.

Table S8. Various nodal SUV_{max} cut-offs (after visual miN+) with corresponding diagnostic accuracy for distinguishing between 0–3 and ≥4 positive LNs in miN+ patients.

Table S9. Proportion of miN+ patients with 0–4 or ≥5 LNM based on various nodal SUV_{max} cut-offs.

Table S10. Univariate logistic regression analyses to assess PSA and PSAd as predictors for pN1 and high-volume LNM disease.

Table S11. Tracer-specific receiver operating characteristic curve analyses for optimal prostate and nodal SUV_{max} cut-off for predicting pN1 disease in miN+ patients.